Acta Radiologica Open
8(6) 1–9

DOI: 10.1177/2058460119853541
journals.sagepub.com/home/arr
SAGE

Correlation between subcutaneous fat measurements in knee MRI and BMI: relationship to obesity and related co-morbidities

Ricardo Hernandez[1], Yara Younan[2], Michael Mulligan[3], Adam D Singer[4], Gulshan B Sharma[5], Monica Umpierrez[4] and Felix M Gonzalez[4]

Abstract

Background: Obesity is a major public health disorder associated with multiple co-morbidities. Knee magnetic resonance imaging (MRI) permits visualization of the subcutaneous fat anatomy, which can be correlated to body mass index (BMI) and obesity-related co-morbidities.

Purpose: This study intends to validate a method of correlating measurements of subcutaneous fat around the distal femur on axial MR images to BMI and obesity-related co-morbidities.

Material and Methods: The most proximal axial slice of each knee MRI was divided into four quadrants. Measurements of the thickest portion of the subcutaneous fat in each quadrant were independently obtained, yielding a value which was assigned the name of the SubCut fat index. The relationship between the SubCut fat index of each quadrant and the patient's BMI was then evaluated. Receiver operating characteristic curves utilizing both the subcutaneous fat in the medial and lateral quadrants as well as BMI were performed with respect to obesity-related co-morbidities.

Results: SubCut fat index measurements in all four quadrants and BMI show the strongest correlation (all four, ANOVA $P < 0.0001$, $r = 0.6$), with subcutaneous fat measurements of the anterior medial ($p < 0.0001$) and posterior medial quadrants ($P = 0.01$). Additionally, BMI and medial quadrants SubCut indices showed strong association with obesity-related co-morbidities including sleep apnea, asthma, diabetes, hypertension, gastroesophageal reflux disease, and osteoporosis.

Conclusion: The SubCut fat index, a marker of distal femur subcutaneous fat on axial MRI, correlates with severity of obesity (BI) and associated obesity-related co-morbidities.

Keywords

Knee, subcutaneous fat, obesity, osteoporosis, asthma

Received 13 November 2018; accepted 29 April 2019

Introduction

Magnetic resonance imaging (MRI) of the knee is one of the most common musculoskeletal radiologic procedures performed today, as its indications are numerous (1). It yields proper assessment of the cruciate and collateral ligaments, making it the preferred imaging modality for evaluating internal derangement of the knee (2). The utility of knee MRI is further demonstrated in its ability to provide detailed imaging of

[1]Philadelphia College of Osteopathic Medicine, Suwanee, GA, USA
[2]Department of General Surgery, University of Kentucky, Lexington, KY, USA
[3]Department of Radiology, University of Maryland Medical Center, Baltimore, MD, USA
[4]Department of Radiology and Imaging Sciences, Emory University Hospital, Atlanta, GA, USA
[5]Department of Psychiatry, Cumming School of Medicine, University of Calgary, Calgary, ALB, Canada

Corresponding author:
Felix M Gonzalez, Emory University Hospital, Department of Radiology and Imaging Sciences, Section of Musculoskeletal Imaging, 59 Executive Park South, 4th Floor, Suite 4009, Atlanta, GA 30329, USA.
Email: felix.m.gonzalez@emory.edu

the subcutaneous fat, a parameter intimately associated with obesity (3–5).

According to the World Health Organization (WHO), obesity is defined as a body mass index (BMI) $\geq$30 kg/m^2 (6). The negative health consequences of obesity and its connection to various morbidities have been understood for many years (7). Obesity, along with other cardiovascular risk factors such as diminished high-density lipoprotein (HDL) cholesterol (<40 mg/dL [1.03 mmol/L] in men and <50 mg/dL [1.29 mmol/L] in women) and elevated fasting plasma glucose (FPG; $\geq$100 mg/dL [5.6 mmol/L]), are part of a cluster of cardiovascular risk factors known as the metabolic syndrome, which has been estimated to affect more than a third of the world's adult population (8). The National Cholesterol Education Program's Adult Treatment Panel III report (ATP III) defined metabolic syndrome as the conglomeration of abdominal obesity, atherogenic dyslipidemia, hypertension (HTN), insulin resistance $\pm$ glucose intolerance, and proinflammatory and prothrombotic states (9).

This study aims to validate a method of correlating measurements of the subcutaneous fat around the distal femur on axial MR images to BMI, as well as predicting obesity associated complications including diabetes, HTN, gastroesophageal reflux disease (GERD), hypothyroidism, chronic obstructive pulmonary disease (COPD), osteoporosis, asthma, anemia, renal function, osteoporosis, and dyslipidemia.

Material and Methods

Patient population

A waiver of informed consent was obtained from the institutional review board for this HIPAA-compliant retrospective study. A database search was performed to identify consecutive individuals who presented for a knee MRI between March of 2012 and April of 2014. Our inclusion criteria focused on skeletally matured patients aged 25–80 years presenting with a chief complaint of "atraumatic" or "non-traumatic" knee pain, which is one of the most common reasons for a knee MRI examination. Our exclusion criteria encompassed patients with conditions that could alter the normal subcutaneous fat anatomy such as previous surgery including arthroplasty, history of infection, eating disorders, and history of recent trauma (traumatic subcutaneous injury may present with swelling that would overestimate normal subcutaneous fat measurements). This information was obtained directly from the medical records. Our patient population included a total of 518 individuals with 528 knees imaged. Demographic information including patients' ages, weights, and BMIs was gathered. Patients' charts were reviewed and data were obtained regarding different laboratory values including hemoglobin/hematocrit, calcium, phosphate, low-density lipoprotein, HDL, blood urea nitrogen, creatinine, glucose, erythrocyte sedimentation rate, and C-reactive protein levels. Lastly, information regarding clinical history of smoking, sleep apnea, COPD, asthma, HLD, diabetes, HTN, GERD, hypothyroidism, osteoporosis, and vitamin D deficiency was collected from medical records. Only laboratory values measured within three months from the MRI examination were considered. Relevant aspects of patients' past medical history were also recorded. We also correlated the presence of co-morbidities to the BMI category (Table 1).

MRI

Out of a total of 528 knees reviewed, 327 knee MRIs were performed using a 1.5-T Philips Eclipse MRI (Andover, MA, USA) at a nearby clinical outpatient site, 129 using a 1.5-T Siemens Avanto (Siemens, Erlangen, Germany) at the university hospital, and 72 using a 3.0-T Siemens Trio magnet located at the university hospital. The studies performed in both the 1.5-T and 3.0-T units used an extremity coil and a standard imaging protocol. The protocol consisted of sagittal T1-weighted spin echo (TR/TE = 600/20 ms), axial and coronal fat-suppressed T2-weighted (T2W) fast spin echo (TR/TE = 4000/70 ms), effective echo train length = 9, axial and coronal proton density (TR/TE = 2000/21 ms), and sagittal STIR (TR/TE/TI = 5000/70/150 ms) imaging sequences with 2–3 excitations. Slice thickness was 3 mm with an interslice gap of 1 mm. Field of view was in the range of 15–18 cm.

Subcutaneous fat measurement

Four observers reviewed each case and measured the thickness of the subcutaneous fat around the distal femur, utilizing the axial fat-suppressed T2W images. Measurement points were taken between the skin surface and the deep fascia at the level of the uppermost axial location, with the thickest subcutaneous fat considered. The uppermost axial plane corresponded to approximately 7–7.5 cm above the lateral joint line (Fig. 1). This distance was determined from the PD FSE coronal view at the midpoint (midpoint in the anteroposterior direction) after tracing an imaginary line bisecting the body of the lateral meniscus in half measuring superiorly 7–7.5 cm and selecting the axial image corresponding to this location. The axial image was divided into four quadrants (anterior medial, anterior lateral, posterior medial, and posterior lateral) as illustrated in Fig. 2.

Table 1. Patient demographics, smoking history, BMI, and serum hemoglobin levels.

	Women	Men	Total
Patients (n)	338	180	518
Age (years)	47.32 ± 13.09	44.02 ± 13.69	46.13 ± 13.39
Knees (n)	340	188	528
Reported history of smoking (n)	131	77	208
Current smoker (n)	77	46	123
Former smoker (n)	54	31	85
BMI (kg/m^2)	33.8 (32.51 ± 7.62)	18 (28.72 ± 5.60)	51.8 (31.20 ± 7.21)
Underweight (n)	4	2	6
Normal (n)	44	46	90
Overweight (n)	92	65	157
Obese (n)	198	67	265
Serum hemoglobin (g/dL)	333 (12.31 ± 1.65)	179 (13.46 ± 2.13)	512 (12.71 ± 1.92)
Anemic (n)	110	58	168
Osteoporosis (n)	50	4	54 (total BMI 33.5 kg/m^2)
Diabetes (n)	61	20	81 (total BMI 35 kg/m^2)
Sleep apnea (n)	20	7	27 (total BMI 38.3 kg/m^2)
COPD (n)	12	6	18 (total BMI 31.9 kg/m^2)
Asthma (n)	49	10	59 (total BMI 34.3 kg/m^2)
GERD (n)	54	13	67 (total BMI 34.8 kg/m^2)
Hypothyroidism	25	4	29 (total BMI 33 kg/m^2)

BMI, body mass index; COPD, chronic obstructive pulmonary disease; GERD, gastroesophageal reflux disease.

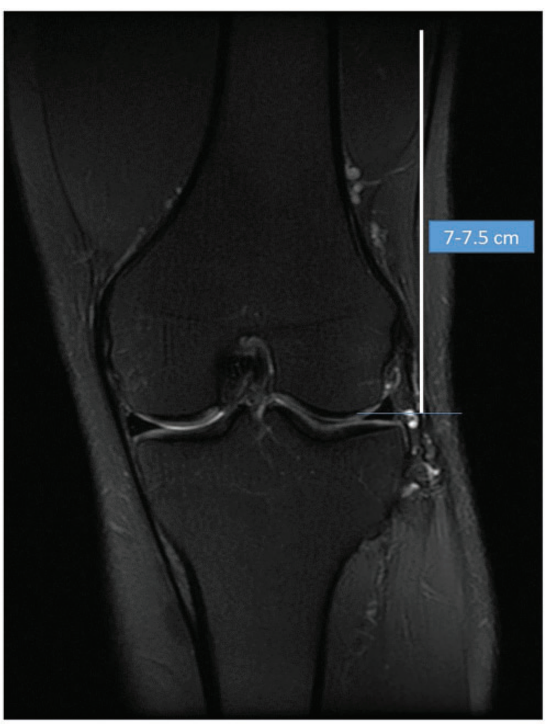

Fig. 1. Coronal knee MRI showing the level at which the axial cut is selected for subcutaneous fat measurements.

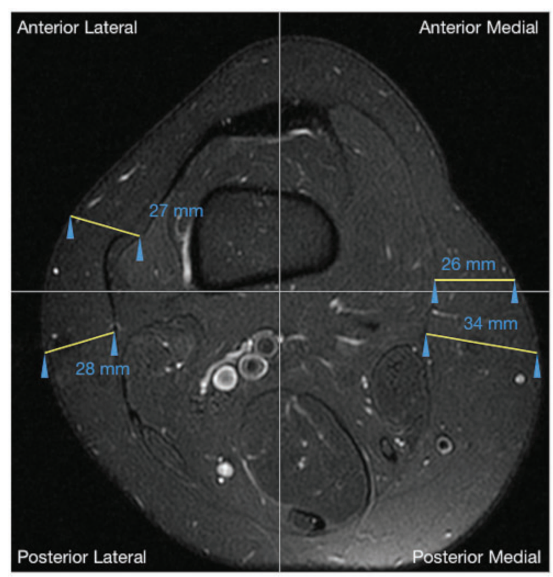

Fig. 2. Axial knee MRI showing the measurement of the thickness of subcutaneous fat in each of the four quadrants.

Four experienced MSK radiologists with a total of 27 years of experience were trained to measure the subcutaneous fat in each quadrant on five different MRI exams. Detailed step-by-step instructions were explained to each of the observers and provided in a written format. Then, to assure reproducibility of the measurements, inter-rater reliability was determined on 15 exams where each reader produced measurements on all four quadrants. For the remaining cases, each observer was assigned a specific quadrant in which to measure the thickness of the subcutaneous fat; therefore, all four quadrants were evaluated. The observers included two fourth-year medical students, a fourth-year radiology resident, and a MSK radiology faculty member with 27 years of experience.

BMI

Categorization of weight class by BMI (kg/m^2) was done using the WHO definitions (2): underweight <18.5; normal = 18.5–24.9; overweight 25–29.9; and obese ≥30.0.

Statistical analysis

All statistical analyses were performed using statistics software (JMP Pro, version 10.2.2, SAS Institute Inc., Cary, NC, USA). Descriptive statistics consisted of means, percentages of sample populations (for continuous and categorical data), and standard deviations (for continuous data). Inter-rater reliability was determined using the intraclass correlation coefficient (ICC) for the SubCut indices in each quadrant using a two-way mixed effects model. A chi-square test was used to determine statistical significance between categorical samples where indicated. Comparison between groups of continuous data was performed using bivariate simple linear regression, testing the model using analysis of variance (ANOVA), and reporting the correlation coefficient (r) and the coefficient of determination (R^2). Between groups of continuous and categorical data, one-way ANOVA, with post-hoc Tukey-Kramer honestly significant difference (HSD), when appropriate, was performed. Contingency analysis with Fisher's exact test or Pearson's chi-square and further two-dimensional and three-dimensional correspondence analysis, when appropriate, was performed for comparisons between categorical data. Any P value < 0.05 was considered statistically significant. Sensitivity and specificity were calculated for observational data; analysis of the receiver operating characteristic (ROC) curve was performed to determine an appropriate cut-off value for continuous observational data. A post-hoc power analysis was conducted using the software G*Power to compute the observed power (10).

Results

Descriptive data

A total of 518 patients with 528 knees imaged were analyzed. Demographic patient data, including age, gender, reported history of smoking, BMI, and serum hemoglobin, are presented in Table 1.

SubCut index and BMI

The SubCut index in all four quadrants was reliably measured by the raters (ICC = 0.999; 95% confidence interval [CI] = 0.998–1; P value < 0.001) on the initial 15 MRI examinations. Bivariate fits of a simple linear regression model for measurements of SubCut index in all four quadrants and BMI were significant (all ANOVA, $P < 0.0001$, r = 0.62, adjusted $R^2 = 0.39$), with measurements of the anterior medial ($P < 0.0001$) and posterior medial quadrants ($P = 0.01$) being the stronger predictors. Figure 3 shows the actual BMI versus predicted BMI values using the above linear regression model. All four SubCut index quadrant measurements showed significant differences ($P < 0.0001$) among all BMI categories (underweight, normal, overweight, and obese). Post-hoc Tukey–Kramer HSD tests showed significant differences between the normal, overweight, and obese categories and SubCut indices in all four quadrants (with P values in the range of 0.025 to <0.0001), except for the posterior lateral quadrant SubCut index, where there was no significant difference found between normal and overweight patients ($P = 0.13$). SubCut indices were significantly different in all four quadrants between the underweight and obese categories (P values in the range of 0.009 to <0.0001), though not between underweight and normal to overweight categories (P values were in the range of 0.097–0.94).

By gender, bivariate fits of a simple linear regression model for measurements of SubCut index in all four quadrants and BMI were significant for both female and male patients (all ANOVA, $P < 0.0001$, female: r = 0.64, adjusted $R^2 = 0.4$, male: r = 0.62, adjusted $R^2 = 0.37$), with measurements of the anterior and posterior medial ($P < 0.0001$) quadrants being significant predictors in women, and the anterior lateral

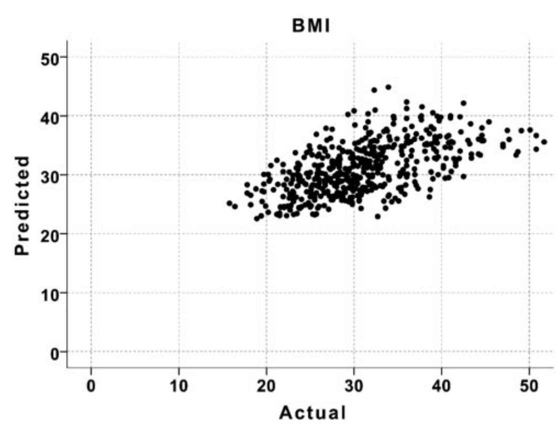

Fig. 3. Actual BMI value plotted vs. predicted BMI value obtained from a linear regression model using SubCut indices from all four quadrants as predictors.

($P = 0.001$) and posterior medial ($P < 0.0001$) quadrant being significant predictors in men. When BMIs were categorized for each gender, all four SubCut index quadrant measurements showed significant differences among BMI categories (P values were in the range of 0.007 to < 0.0001 for all).

Analysis of the ROC curve utilizing the anterior and posterior medial quadrants of patients in the obese category yielded an area under the curve (AUC) of 0.7904 and 0.7828, respectively. The sensitivity of using a cut-off value of 20 mm in the posterior medial quadrant of obese patients is 68.73%, while the specificity is 74.29%. Raising the cut-off value to 25 mm in the posterior medial quadrant, the sensitivity for detecting obesity increases to 78.13% and the specificity decreases to 69.28%. Further, raising the cut-off value to 30 mm in the posterior medial quadrant follows the same trend, increasing the sensitivity for detecting obesity to 83.70% while decreasing the specificity to 60.21%.

Finally, analysis of the ROC curves utilizing both medial and lateral quadrants as well as BMI was performed with respect to obesity-related co-morbidities. BMI was shown to outperform medial and lateral SubCut indices in most categories, with sleep apnea having the highest AUC of 75 with a threshold of 31.55. Medial SubCut indices performed better than lateral. Tables 5–7 show the ROC analysis results using BMI, posterior medial SubCut index, and anterior medial SubCut index, respectively.

BMI and statistically insignificant co-morbidities

There was no statistically significant difference ($P = 0.05$) between the categories of BMI and smoking by one-way ANOVA (Table 2). No statistically significant difference ($P = 0.77$) was found between mean BMI for those patients with a history of COPD (31.92 kg/m^2) and those without a history of COPD (31.18 kg/m^2) by independent samples t-test with unequal variance (Levene's test, $P = 0.003$). There was also no correlation ($P = 0.2$) between mean BMI for those with a history of HLD (32.60 kg/m^2) and those without a history of HLD (31.08 kg/m^2) by independent samples t-test with equal variance (Levene's test, $P = 0.26$). Additionally, there was no statistically significant difference ($P = 0.28$) between mean BMI for those with a history of hypothyroid (32.62 kg/m^2) and those without a history of hypothyroid (31.12 kg/m^2) by independent samples t-test with equal variance (Levene's test, $P = 0.62$). ROC analysis using BMI as the predictor found no significant difference between AUC and 50% when discriminating participants based on their status of smoking, COPD history, HLD history, and hypothyroidism.

BMI and statistically significant co-morbidities

The observed power (91.5%) for significant co-morbidities were $> 99\%$, with the exception of sleep apnea (Table 3).

Sleep apnea: A statistically significant difference ($P < 0.001$) was found between mean BMI for those with a history of sleep apnea (38.28 kg/m^2) and those without a history of sleep apnea (30.80 kg/m^2) by independent samples t-test with unequal variance (Levene's test, $P = 0.05$). Analysis of the ROC curve for the patients with sleep apnea yielded an AUC of 0.748. The sensitivity of detecting sleep apnea using a cut-off BMI value of 31.55 kg/m^2 is 81.5%, while the specificity is 60%.

History of asthma*:* Regarding patients with a reported history of asthma, a statistically significant difference ($P = 0.001$) between mean BMI for those with a history of asthma (34.26 kg/m^2) and those without a history of asthma (30.80 kg/m^2) by independent samples t-test with equal variance (Levene's test, $P = 0.34$) was seen. Analysis of the ROC curve for the patients with history of asthma yielded an AUC of 0.633. The sensitivity of detecting asthma using a cut-off BMI value of 29.85 kg/m^2 is 71.2%, while the specificity is 49.7%.

History of diabetes: Furthermore, a statistically significant difference ($P = 0.000$) between mean BMI and those with a history of diabetes (34.95 kg/m^2) and those without a history of diabetes (30.49) by independent samples t-test with unequal variance (Levene's test $p=0.04$) was seen. Analysis of the ROC curve for the patients with history of diabetes yielded an AUC of 0.674. The sensitivity of detecting diabetes using a cutoff BMI value of 30.75 is 70.4%, while the specificity is 57.5%.

History of HTN: When it came to comparing mean BMI and history of HTN, a statistically significant difference ($P < 0.001$) was seen in those patients with a history of HTN (33.61 kg/m^2) in comparison to those without a history of HTN (29.91 kg/m^2) by independent samples t-test with unequal variance (Levene's test, $P = 0.02$). Analysis of the ROC curve for the patients with history of HTN yielded an AUC of 0.654. The sensitivity of detecting HTN using a cut-off BMI value of 31.185 kg/m^2 is 62.5%, while the specificity is 65.3%.

History of GERD: There is a statistically significant difference ($p < 0.001$) between mean BMI for those with a history of GERD (34.76 kg/m^2) and those without a history of GERD (30.66 kg/m^2) by independent samples t-test with unequal variance (Levene's test, $P = 0.01$). Analysis of the ROC curve for the patients with history of GERD yielded an AUC of 0.638. The sensitivity of detecting GERD using a cut-off BMI

Table 2. Summary of BMI's discrimination of specific co-morbidities.

Significant discrimination*	Non-significant discrimination	ROC AUC (%); *P* value
Sleep apnea	Reported smoking history	55.9; 0.37
Asthma	COPD	49.6; 0.95
Diabetes	HLD	58.4; 0.08
HTN	Hypothyroidism	54.8; 0.39
GERD		
Osteoporosis		

*Refer to Table 5 for ROC AUC.
ROC, receiver operating characteristic; AUC, area under the curve; COPD, chronic obstructive pulmonary disease; HLD, high-density lipoprotein; HTN, hypertension; GERD, gastroesophageal reflux disease.

value of 30.85 kg/m^2 is 61.2%, while the specificity is 55.4%.

History of osteoporosis: Lastly, a statistically significant difference ($P = 0.03$) was observed between mean BMI for those with a history of osteoporosis (33.17 kg/m^2) and those without a history of osteoporosis (30.97 kg/m^2) by independent samples t-test with equal variance (Levene's test, $P = 0.64$). Analysis of the ROC curve for the patients with history of osteoporosis yielded an AUC of 0.590. The sensitivity of detecting osteoporosis using a cut-off BMI value of 30.75 kg/m^2 is 61.1%, while the specificity is 54.7%.

Table 3. Analysis of ROC curve using BMI in relation to co-morbidities.

Co-morbidity	BMI threshold (kg/m^2)	Sensitivity (%)	Specificity (%)	Area under ROC curve ± SE (%)	95% CI (%)	*P* value
Sleep apnea	31.55	81.5	60	75 ± 5	65–85	<0.001
Asthma	29.85	71.2	49.7	63.3 ± 3.6	56.3–70.4	0.001
Diabetes	30.75	70.4	57.5	67.4 ± 3.3	60.9–73.9	<0.001
HTN	30.45	66.5	61	65.4 ± 2.6	60.3–70.5	<0.001
GERD	30.25	65.7	52.6	63.8 ± 3.6	56.7–70.9	<0.001
Osteoporosis	30.59	63	53.8	59 ± 4	51.1–66.9	0.03

BMI, body mass index; SE, standard error; CI, confidence interval; ROC, receiver operating characteristic; HTN, hypertension; GERD, gastroesophageal reflux disease.

Table 4. Analysis of ROC curve using posterior medial SubCut index in relation to co-morbidities.

Co-morbidity	SubCut posterior medial threshold (mm)	Sensitivity (%)	Specificity (%)	Area under ROC curve ± SE (%)	95% CI (%)	*P* value
Sleep apnea	25.15	63.0	59.4	66.8 ± 5.8	55.5–78.0	0.003
Asthma	24.4	71.2	59.2	64.4 ± 3.6	57.4–71.4	<0.001
Diabetes	24.65	60.5	59.4	62.6 ± 3.3	56.1–69.1	<0.001
HTN	23.1	60.2	59.6	60.8 ± 2.6	55.6–65.9	<0.001
GERD	24.4	61.2	58.2	63.6 ± 3.4	56.9–70.2	<0.001
Osteoporosis	23.45	61.1	55.4	63.8 ± 3.7	56.6–71.1	0.001

BMI, body mass index; SE, standard error; CI, confidence interval; ROC, receiver operating characteristic; HTN, hypertension; GERD, gastroesophageal reflux disease.

Table 5. Analysis of ROC curve using anterior medial SubCut index in relation to co-morbidities.

Co-morbidity	SubCut anterior medial threshold (mm)	Sensitivity (%)	Specificity (%)	Area under ROC curve ± SE (%)	95% CI (%)	*P* value
Sleep apnea	18.05	66.7	55.6	64.9 ± 5.0	55.1–74.6	0.009
Asthma	19.45	67.8	61.6	66.3 ± 3.6	59.2–73.4	<0.001
Diabetes	18.15	60.5	58.2	61.9 ± 3.3	55.4–68.4	0.001
HTN	16.05	60.8	51.3	60.5 ± 2.6	55.3–65.7	<0.001
GERD	18.05	61.2	56.8	64.3 ± 3.5	57.5–71.1	<0.001
Osteoporosis	17.95	72.2	56.9	67.7 ± 3.1	61.6–73.7	<0.001

BMI, body mass index; SE, standard error; CI, confidence interval; ROC, receiver operating characteristic; HTN, hypertension; GERD, gastroesophageal reflux disease.

Table 6. Performance comparison of BMI and SubCut index in all four quadrants in relation to co-morbidities using analysis of ROC curve.

		Co-morbidities					
Measures	ROC analysis	Sleep apnea	Asthma	Diabetes	HTN	GERD	Osteoporosis
BMI	Area under ROC curve ± SE (%); 95% CI (%); *P* value	75 ± 5; 65–85; < 0.001	63.3 ± 3.6; 56.3–70.4; 0.001	67.4 ± 3.3; 60.9–73.9; < 0.001	65.4 ± 2.6; 60.3–70.5; < 0.001	63.8 ± 3.6; 56.7–70.9; < 0.001	59 ± 4; 51.1–66.9; 0.03
SubCut posterior medial	Area under ROC curve ± SE (%); 95% CI (%); *P* value	68.8 ± 5.8; 55.5–78; 0.003	64.4± 3.6; 57.4–71.4; < 0.001	62.6 ± 3.3l; 56.1–69.1; < 0.001	60.8 ± 2.6; 55.6–65.9; < 0.001	63.6 ± 3.4; 56.9–70.2; < 0.001	63.8 ± 3.7; 56.6–71.1; 0.001
SucCut anterior medial	Area under ROC curve ± SE (%); 95% CI (%); *P* value	64.9 ± 5.0; 55.1–74.6; 0.009	66.3 ± 3.6; 59.2–73.4; < 0.001	61.9 ± 3.3; 55.4–68.4; 0.001	60.5 ± 2.6; 55/3–65/7; < 0.001	64.3 ± 3.5; 57.5–71.1; < 0.001	67.7 ± 3.1; 61.6–73.7; < 0.001
SubCut anterior lateral	Area under ROC curve ± SE (%); 95% CI (%); *p* value	60.1 ± 5.0; 50.7–69.4; 0.08	58.2 ± 3.8; 50.7–65.7; 0.04	58.4 ± 3.3; 51.9–64.8; 0.02	59.3 ± 2.7; 54.1–64.5; 0.001	63.5 ± 3.4; 56.7–70.2; < 0.001	65.3 ± 3.3; 58.8–71.7; < 0.001
SubCut posterior lateral	Area under ROC curve ± SE (%); 95% CI (%); *P* value	54.9 ± 5.1; 45–64.9; 0.39	60.9 ± 4.2; 52–69; 0.01	55.3 ± 3.3; 48.8–61.8; 0.13	55.8 ± 2.7; 50.6–61; 0.03	57.7 ± 3.6; 50.7–64.8; 0.04	59.2 ± 3.5; 52.3–66; 0.03

BMI, body mass index; SE, standard error; CI, confidence interval; ROC, receiver operating characteristic; HTN, hypertension; GERD, gastroesophageal reflux disease.

Discussion

This study confirms a statistically significant relationship between subcutaneous fat measurements at the level of the most proximal axial image on knee MRIs and BMI. Although the correlation in all four quadrants proved to be significant ($P < 0.0001$), the SubCut index (thickest subcutaneous fat measurement) in the posterior medial quadrant was found to have the strongest correlation with BMI in both male and female patients, meaning the thickest subcutaneous fat measurement in this knee quadrant predicts BMI the best.

The findings presented in this study are becoming increasingly more relevant as obesity has become a problem of epidemic proportions (Tables 4 and 5). According to the CDC National Center for Health Statistics (NCHS), more than one-third (36.5%) of adults in the United States are classified as obese (11). Interestingly, the prevalence of obesity in our patient population was 51%. The apparent increase in the prevalence of obesity can be attributed to the specific study's patient population presenting to our clinic with knee pain. Obese patients are more likely to present with knee pain due to increased mechanical load and other biomechanical factors (12).

One of the objectives of the study was to assess whether the BMI or the SubCut index would correlate with obesity co-morbidities (Table 6). BMI and SubCut fat index correlated well with the presence of obesity-associated co-morbidities including sleep apnea, asthma, diabetes, HTN, GERD, and osteoporosis. However, BMI outperformed the subcutaneous anterior medial and posterior medial fat measurements for detection of sleep apnea (sensitivity = 81.5%), diabetes (sensitivity = 70.4%), HTN (sensitivity = 66.5%), and GERD (sensitivity = 65.7%) within a BMI range of 30.3–31.6 kg/m^2. On the other hand, the SubCut posterior medial index performs as well as BMI in screening for asthma utilizing 24.4 mm as a subcutaneous fat threshold (upper limits of normal), while the SubCut anterior medial index outperforms BMI in detection of osteoporosis at a threshold of 18 mm (sensitivity = 72.2%). One relevant point is that the SubCut indices did not significantly change among individuals with and without the different co-morbidities (Table 7). This is significant that in patients with normal body weight, the anteromedial subcutaneous fat measurement identifies patients with osteoporosis in two-thirds of the time in our patient population. It is difficult to predict how these observations will translate to the general population. One of the main points of this work is to point out these correlations worth studying at a greater scale.

Of those co-morbidities which our study showed to be significantly correlated with obesity, we found the

Table 7. Multivariate general linear model analysis predicting SubCut index values depending on BMI categories with co-morbidities as covariates.

		SubCut index values in all four quadrants (mm) (mean ± SD)			
Co-morbidity	Present	Posterior medial	Anterior medial	Anterior lateral	Posterior lateral
Sleep apnea	Yes	30.6 ± 12.4	24.1 ± 12.1	17.1 ± 7.2	15.8 ± 7.5
	No	23.3 ± 10.2	18 ± 11.4	14.8 ± 8.6	15.1 ± 9.2
	P value	0.15	0.69	0.37	0.19
Asthma	Yes	28 ± 9.8	23.6 ± 11	16.9 ± 8.5	18.6 ± 10.7
	No	23.1 ± 10.4	17.6 ± 11.4	14.7 ± 8.5	14.7 ± 8.7
	P value	0.03	0.01	0.45	0.01
Diabetes	Yes	27.5 ± 10.9	21.9 ± 11.2	16.9 ± 8.4	15.9 ± 8.3
	No	23 ± 10.2	17.6 ± 11.5	14.6 ± 8.5	15 ± 9.2
	P value	0.34	0.6	0.85	0.32
HTN	Yes	26.1 ± 10.4	20.7 ± 11.1	16.7 ± 8.7	15.9 ± 8.5
	No	22.4 ± 10.2	17 ± 11.6	14 ± 8.3	14.8 ± 9.4
	P value	0.56	0.81	0.55	0.58
GERD	Yes	27.7 ± 9.7	23 ± 11.2	18.3 ± 8.6	16.8 ± 8.6
	No	23.1 ± 10.4	17.6 ± 11.4	14.4 ± 8.4	14.9 ± 9.1
	P value	0.14	0.05	0.05	0.39
Osteoporosis	Yes	28.1 ± 9.8	23.8 ± 9.3	18.6 ± 7.9	16.5 ± 7.2
	No	23.2 ± 10.4	17.7 ± 11.6	14.5 ± 8.5	15 ± 9.3
	P value	0.04	0.01	0.02	0.47

P value adjusted for multiple comparison shows significant covariates.
BMI, body mass index; SD, standard deviation; HTN, hypertension; GERD, gastroesophageal reflux disease.

relatively high incidence of osteoporosis in obese patients especially interesting. Osteoporosis is a skeletal disease characterized by reduced bone strength leading to an increased risk of fractures (13). It tends to affect more women than men and is typically seen in patients aged $\geq$ 65 years (14,15). Studies have shown, however, that a higher BMI is associated with a lesser osteoporotic risk, with the belief being that a greater adaptive bone mass is needed to accommodate the larger body mass (16). Additionally, it has been postulated that the estrogen produced by adipose tissue inhibits bone resorption by directly inhibiting osteoclastic activity (17). In our study, 94% of our osteoporotic patients were women (46 out of 49) with an average age of 52.6 years, which is younger than the average presenting age for this disease. The SubCut index may be utilized as a triage screen for osteoporosis.

BMI has associated sensitivities in the range of 63–81.5% and specificity in the range of 50–61%. The SubCut index has sensitivities in the range of 60.2–71.2% while the specificity falls within a range of 55.4–59.6%. It should be noted that the prevalence of a disease may be different in different clinical settings. For example, the pre-test probability for a positive test would be expected to be higher when a patient consults a specialist than when they consult a general practitioner. We propose the use of BMI and SubCut index as triage tests to exclude presence of disease.

Our study is limited by its retrospective nature and the lack of longitudinal follow-up and outcome data. Our patient population consists mostly of overweight women. In addition, the data acquired were from a single center, limiting our findings to reflect only local pathology. Follow-up examinations were not performed, which have the potential to substantially increase the number of patients examined with related co-morbidities. Furthermore, data collected from patients, such as history of smoking, were self-reported, which have the possibility of recall bias. This study can serve as a platform to a future multi-center approach that would allow patient follow-ups in a longitudinal fashion.

The relative ease and cost-effectiveness of this simple measurement further enhances the value of care provided to the patient presenting with knee pain requiring MRI. Overall, our data suggest an association between the posterior medial SubCut index and BMI regardless of gender in addition to its use in the screening of patients with history of sleep apnea, asthma, diabetes, HTN, GERD, and osteoporosis.

In conclusion, the use of the SubCut index paves a way for more specific recommendations to screen for patients who are at risk of developing diseases related to obesity, thereby impacting clinical outcomes by utilizing information currently wasted on knee MRI examinations. We hope that this study becomes a platform for other studies to be performed to realize the full potential of the method discussed in this paper in the detection of obesity-related co-morbidities that are usually screen for in patients aged > 60 years but do not fall in the screening radar in younger patients.

Acknowledgements

The authors thank Erica Monfred and Terence Anguh for their contributions with the subcutaneous fat measurements.

Declaration of conflicting interests

The authors declared no potential conflicts of interest with respect to the research, authorship, and/or publication of this article.

Funding

The author(s) received no financial support for the research, authorship, and/or publication of this article.

ORCID iD

Felix M Gonzalez https://orcid.org/0000-0002-3214-4813

References

1. American College of Radiology. ACR-SPR-SSR Practice Parameter for the Performance and Interpretation of Magnetic Resonance Imaging (MRI) of the Knee. 2015 Resolution No. 6. Reston, VA: ACR, 2015. Available at: https://www.acr.org/-/media/ACR/Files/Practice-Parameters/mr-knee.pdf?la=en (accessed 17 June 2017).
2. Vohra S, Arnold G, Doshi S, et al. Normal MR imaging anatomy of the knee. *Magn Reson Imaging Clin N Am* 2011;19:637–653.
3. Hong Kuan K, Donnellan J, Ryan D, et al. Correlation between subcutaneous knee fat thickness and chondromalacia patellae on magnetic resonance imaging of the knee. *Can Assoc Radiol J* 2013;64:182–186.
4. Diepold J, Ruhdorfer A, Dannhauer T, et al. Sex-differences of the healthy infra-patellar (Hoffa) fat pad in relation to intermuscular and subcutaneous fat content – Data from the Osteoarthritis Initiative. *Ann At* 2015;200:30–36.
5. Trevor G, Carey F, Cahir J, et al. Fluid signal changes around the knee on MRI are associated with increased volumes of subcutaneous fat: a case-control study. *BMC Musculosket Disord* 2016;17:487.
6. World Health Organization. *Obesity: preventing and managing the global epidemic*. Geneva: WHO, 2000. Available at: http://www.who.int/nutrition/publications/obesity/WHO_TRS_894/en/ (accessed 17 June 2017).
7. National Health, Lung, and Blood Institute. Managing overweight and obesity in adults: systematic evidence review from obesity expert panel. Washington, DC: NIH, 2013. Available at: https://www.nhlbi.nih.gov/sites/default/files/media/docs/obesity-evidence-review.pdf (accessed 18 June 2017).
8. Moore JX, Chaudhary N, Akinyemiju T. Metabolic syndrome prevalence by race/ethnicity and sex in the United States, National Health and Nutrition Examination Survey, 1988–2012. *Prev Chronic Dis* 2017;14:160–287.
9. Beilby J. Definition of metabolic syndrome: report of the National Heart, Lung, and Blood Institute/American Heart Association Conference on Scientific Issues Related to Definition. *Clin Biochem Rev* 2004;25:195–198.
10. Faul F, Erdfelder E, Buchner A, et al. Statistical power analyses using G*Power 3.1: tests for correlation and regression analyses. *Behav Res Methods* 2009;41:1149–1160.
11. Ogden CL, Carroll MD, Fryar CD, et al. Prevalence of obesity among adults and youth: United States, 2011–2014. *NCHS Data Brief* 2015;219:1–8.
12. Hofmann S, Kramer J, Vakil-Adli A, et al. Painful bone marrow edema of the knee: differential diagnosis and therapeutic concepts. *Orthop Clin North Am* 2004;35:321–333.
13. Aspray TJ, Hill TR. Osteoporosis and the ageing skeleton. *In Biochemistry and Cell Biology of Ageing: Part II Clinical Science* 2019; 91: 453–476.
14. World Health Organization. *Assessment of fracture risk and its application to screening for postmenopausal osteoporosis: technical report series 843*. Geneva: WHO, 1994. Available at: http://www.who.int/chp/topics/Osteoporosis.pdf (accessed 17 June 2017).
15. Looker C, Sarafrazi N, Fan B, et al. Trends in osteoporosis and low bone mass in older US adults, 2005–2006 through 2013–2014. *Osteoporos Int* 2017;28:1979–1988.
16. Zhao J, Liu J, Liu Y, et al. Relationship of obesity with osteoporosis. *J Clin Endocrinol Metab* 2007;92:1640–1646.
17. Kameda T, Mano H, Yuasa T, et al. Estrogen inhibits bone resorption by directly inducing apoptosis of the bone-resorbing osteoclasts. *J Exp Med.* 1997;186:489–495.